CuticleTrace: A toolkit for capturing cell outlines of leaf cuticle with implications for paleoecology and paleoclimatology

Benjamin A. Lloyd[1,2], Richard S. Barclay[3], Regan E. Dunn[4], Ellen D. Currano[5], Ayuni I. Mohamaad[5,6], Kymbre Skersies[5], and Surangi W. Punyasena[7].

[1]Department of Earth and Space Sciences, University of Washington, Seattle, WA 98195;
[2]Smithsonian Environmental Research Center, Smithsonian Institution, Edgewater, MD, 21037;
[3]Department of Paleobiology, National Museum of Natural History, Smithsonian Institution, Washington, D.C. 20013;
[4]La Brea Tar Pits & Museum, Natural History Museums of Los Angeles County, Los Angeles, CA 90036;
[5]Department of Botany, University of Wyoming, Laramie, WY 82071;
[6]Department of Geological Sciences, University of Florida, Gainesville, FL 32611;
[7]Department of Plant Biology, University of Illinois at Urbana-Champaign, Urbana, IL 61801.

Abstract

1. The accurate and efficient characterization of the leaf epidermis is important to efforts to disentangle the relationships between plant morphology, evolutionary history, and growth environment. Epidermal cells form the surface through which light capture and gas exchange takes place, serving as the primary interface between plants and their environment. Epidermal pavement cells exhibit highly variable morphology, influenced by both phylogeny and environment. This variation is of interest to a broad range of plant biologists, including paleobotanists, systematists, and physiologists. Existing automated methods for epidermal pavement cell segmentation are limited in their application and have not been widely adopted. The labor needed to generate hand-traced datasets have circumscribed the use of epidermal cell morphology in paleoenvironmental, phylogenetic, and phenomic research.
2. To streamline epidermal cell analysis, we developed CuticleTrace, a suite of FIJI and R-based functions that streamlines and automates the segmentation and measurement of epidermal pavement cells across a wide range of cell morphologies and image qualities. To test CuticleTrace's effectiveness, we compared CuticleTrace measurements to those from alternate automated methods and expert and undergraduate hand-tracings across a taxonomically diverse 50-image dataset of variable image qualities.
3. CuticleTrace measurements consistently aligned more closely with expert hand-traced measurements than expert measurements did with undergraduate hand-tracings and alternate automated measurements. We observed ~93% statistical agreement between CuticleTrace and expert measurements.
4. CuticleTrace is broadly applicable, modular, and customizable, and integrates data visualization and cell shape measurement with image segmentation, lowering the barrier to high-throughput studies of epidermal morphology by vastly decreasing the labor investment required to generate high-quality cell shape datasets.

Keywords

Cell shape, high-throughput phenotyping, image processing, image segmentation, leaf area index, leaf epidermis, paleobotany, paleoecology.

1 | Introduction

The accurate, consistent, and efficient characterization of the leaf epidermis is key to advancing our understanding of the relationships of plants to their environments and evolutionary histories. The morphology and arrangement of leaf epidermal cells varies significantly across different environmental conditions and taxonomic groups (Kürschner, 1997; Royer, 2001; Vőfély et al., 2019). These relationships have been used to constrain paleoenvironmental conditions such as atmospheric CO_2 concentration (McElwain & Chaloner, 1996; Royer, 2001) and canopy structure (Bush et al., 2017; Dunn et al., 2015; Milligan et al., 2021) and to enhance taxonomic resolution of paleofloras (e.g. Strömberg, 2011). In crop science, phenomics links high-throughput phenotyping of leaf epidermal characters (cell size, shape, number, etc.) with genomics to breed plants with idealized physiological traits (Zhao et al., 2019).

Efforts to automate leaf epidermal measurement have met differing levels of success. Stomata can be efficiently identified from microscope images (e.g. Fetter et al., 2019; Li et al., 2022), but the accurate characterization of epidermal pavement cell morphologies remains limited to specific taxa or imaging techniques (Li et al., 2022; Möller et al., 2017). As a result, hand-tracing has remained the most viable option for characterizing epidermal pavement cell morphology in most cases (e.g. Brown & Jordan, 2023; Vőfély et al., 2019). However, hand-tracing is a slow and tedious process, with cell-outline quality highly dependent upon both the tools used for tracing (mouse, stylus, tablet, desktop computer) and the experience level and conscientiousness of the tracer. The high labor requirement of hand tracing—and the non-standardized measurements that result—imposes a barrier to the use of cell shape in multiple disciplines. Regardless, hand-traced datasets have been part of high-impact studies studying cell shape, growth environment, and evolutionary history (Bush et al., 2017; Dunn et al., 2015; Vőfély et al., 2019). These studies demonstrate how cell shape datasets enable significant developments in paleobotany and evolutionary biology.

We developed the CuticleTrace toolkit to streamline and automate the tracing and measurement of epidermal pavement cells across a wide variety of taxa, image qualities, and image preparations. Our easily fine-tuned open-source workflow uses the freeware software FIJI (Schindelin et al., 2012) and R Statistical Software (R) (R Core Team, 2022). CuticleTrace generates large cell-shape datasets from images of leaf cuticle or epidermis. Cell-tracing is fast, consistent, and reproduces expert-level measurements.

2 | CuticleTrace Description

The CuticleTrace workflow consists of four steps. First, users determine appropriate batch-processing inputs with the "Single Image Processor" FIJI macro (Fig. 1b). Second, users batch-process images and measure cells with the "Batch Generate ROIs" and "Batch Measure (Different Scales)" FIJI macros, which generate (1) thresholded and skeletonized binary images (Fig. 1f-g), (2) sets of files recording individual cell shapes known as "regions of interest" (ROIs; Fig. 1i), and (3) shape parameter measurements associated with each ROI (Fig. 1j). Third, resulting cell measurements are filtered with median statistics by the "CuticleTrace Data Filtration" R notebook (Fig. 1k). Last, users can visualize the effects of data filtration with the "Batch Overlay" FIJI macro (Fig. 1j).

An illustrated manual for installation and use of FIJI and R tools is available in the supporting information (**Methods S1**). A video tutorial is available online [link available after acceptance] and all software is documented on the CuticleTrace GitHub repository (https://github.com/benjlloyd/CuticleTrace).

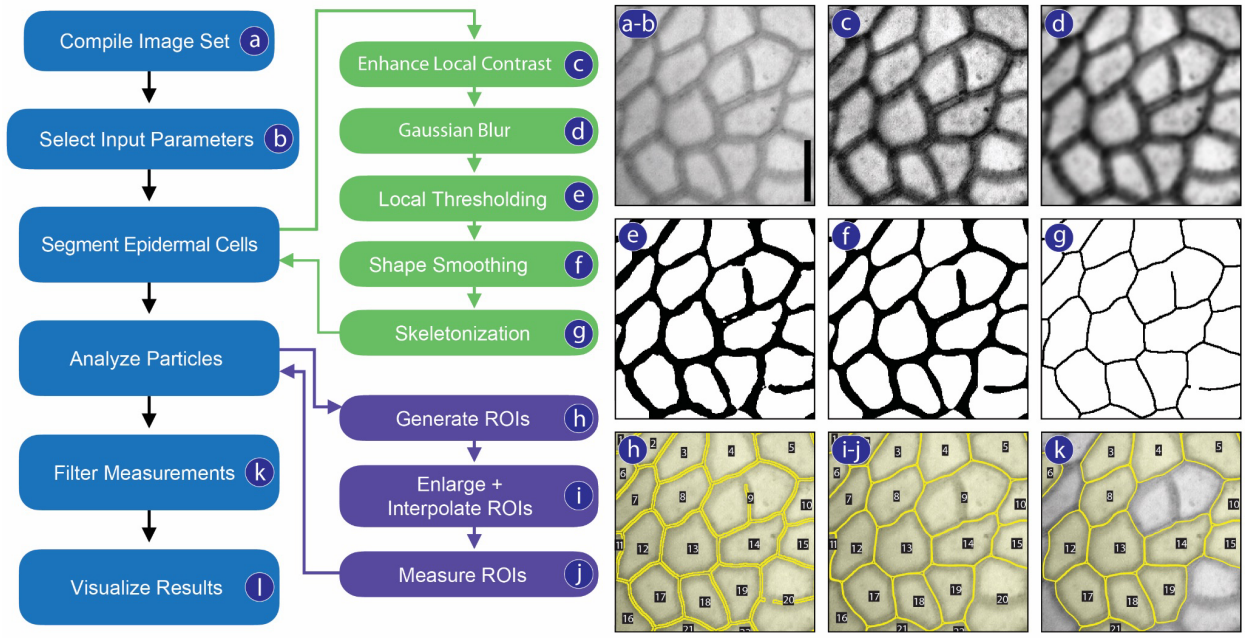

Fig. 1 Processing workflow for the CuticleTrace toolkit (left), illustrated on *Castanea pumila* (Fagaceae, FLMNH00115). Scale bar is 10µm. See text for further explanation.

2.1 | Determination of Batch Processing Inputs

Both the "Single Image Processor" and "Batch Generate ROIs" macros apply seven user inputs to images. "Single Image Processor" works with an open image, while "Batch Generate ROIs" processes all images in an image set. Each user input sets the parameters for different image processing operations. Before batch-processing, users must first determine the appropriate input parameters on a small subset of images using the "Single Image Processor" macro. The selection of appropriate input parameters is extremely important to ensure accurate results (Fig. 2).

For both macros, users select:

1. Whether cell walls are dark on a light background, or light on a dark background
2. The standard deviation of Gaussian blur (Fig. 1c)
3. The automated local thresholding algorithm (Fig. 1d, Fig. 2)
4. The initial local thresholding radius (Fig. 1d)
5. The range of sizes (in pixels squared) of all cells expected in the image set (Fig. 1d)
6. The percentage of Fourier descriptors to retain during shape smoothing (Fig. 1e)
7. The scale (in pixels/unit) of all images in the image set (Fig. 1i)

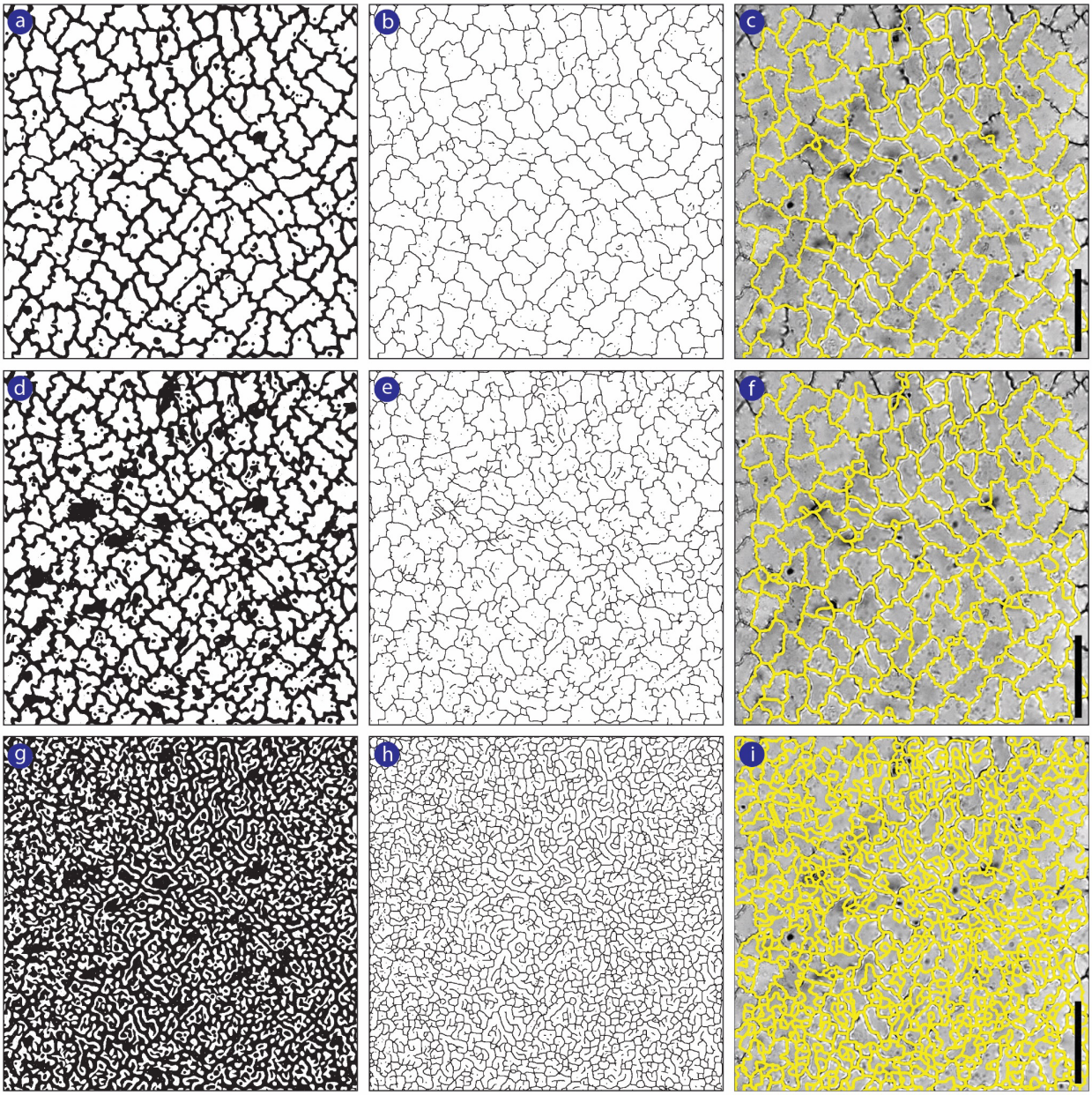

Fig. 2 The effect of thresholding **(a, d, g)** on skeletonization **(b, e, h)** and unfiltered ROI sets **(c, f, i)**, demonstrated on *Talisia princeps* - Sapindaceae, FLMNH00443. The image is thresholded by **(a-c)** Sauvola local thresholding (ideal), **(d-f)** Bernsen local thresholding (satisfactory), and **(g-i)** NiBlack local thresholding (ineffective). Scale bars are 50µm.

2.2 | Image Processing and Measurement

The "Batch Generate ROIs" macro outputs thresholded and skeletonized binary images, and unfiltered (enhanced and interpolated) ROI sets of all images in a directory (Fig. 1c-i). Users may also elect to output measurements of ROI shape parameters if all images have the same scale, or use "Batch Measure (Different Scales)" to measure ROIs of images with differing scales (Fig. 1j, Table 1). These unfiltered ROI sets and measurement files may then be brought directly into the "CuticleTrace Data Filtration" R Notebook for statistical filtration.

Table 1. Descriptions or equations of all shape parameters measured by CuticleTrace.

Measurement Parameter	Description or Equation
Area	The area of an ROI.
Perimeter	The length of the outside boundary of an ROI.
Bounding Rectangle	The X-Y coordinates and dimensions of the smallest rectangle that encloses an ROI.
Fit Ellipse	The dimensions and orientation of an ellipse fit to an ROI.
Feret's Diameter	The longest distance between any two points on the ROI boundary.
Minimum Feret's Diameter	The shortest distance between any two points on the ROI boundary.
Circularity	$4\pi * \frac{[Area]}{[Perimeter]^2}$
Aspect Ratio	$\frac{[Major\ Axis\ of\ Fit\ Ellipse]}{[Minor\ Axis\ of\ Fit\ Ellipse]}$
Roundness	$4 * \frac{[Area]}{\pi * [Major\ Axis\ of\ Fit\ Ellipse]^2}$
Solidity	$\frac{[Area]}{[Area\ of\ Convex\ Hull]}$
Undulation Index	$\frac{[Perimeter]}{2\pi * \sqrt{[Area]/\pi}}$

2.3 | Data Filtration

The ROIs produced by the CuticleTrace FIJI analysis pipeline will inevitably include partial cells, multiple cells, vein cells, or non-cuticle image artifacts (e.g., slide background, debris). The "CuticleTrace Data Filtration" R notebook removes these erroneous data points by excluding ROIs with measurements outside one or two median absolute deviations (MADs) from each image's median area, perimeter, circularity, aspect ratio, roundness, and solidity (Table 1). The notebook then creates new ROI sets of the remaining ROIs post-filtering (Fig. 3). We use the median as our reference point, as unfiltered measurements are non-normally distributed (Fig. 4). This approach retains ROIs that capture the central tendency of each specimen's epidermal pavement cell morphology.

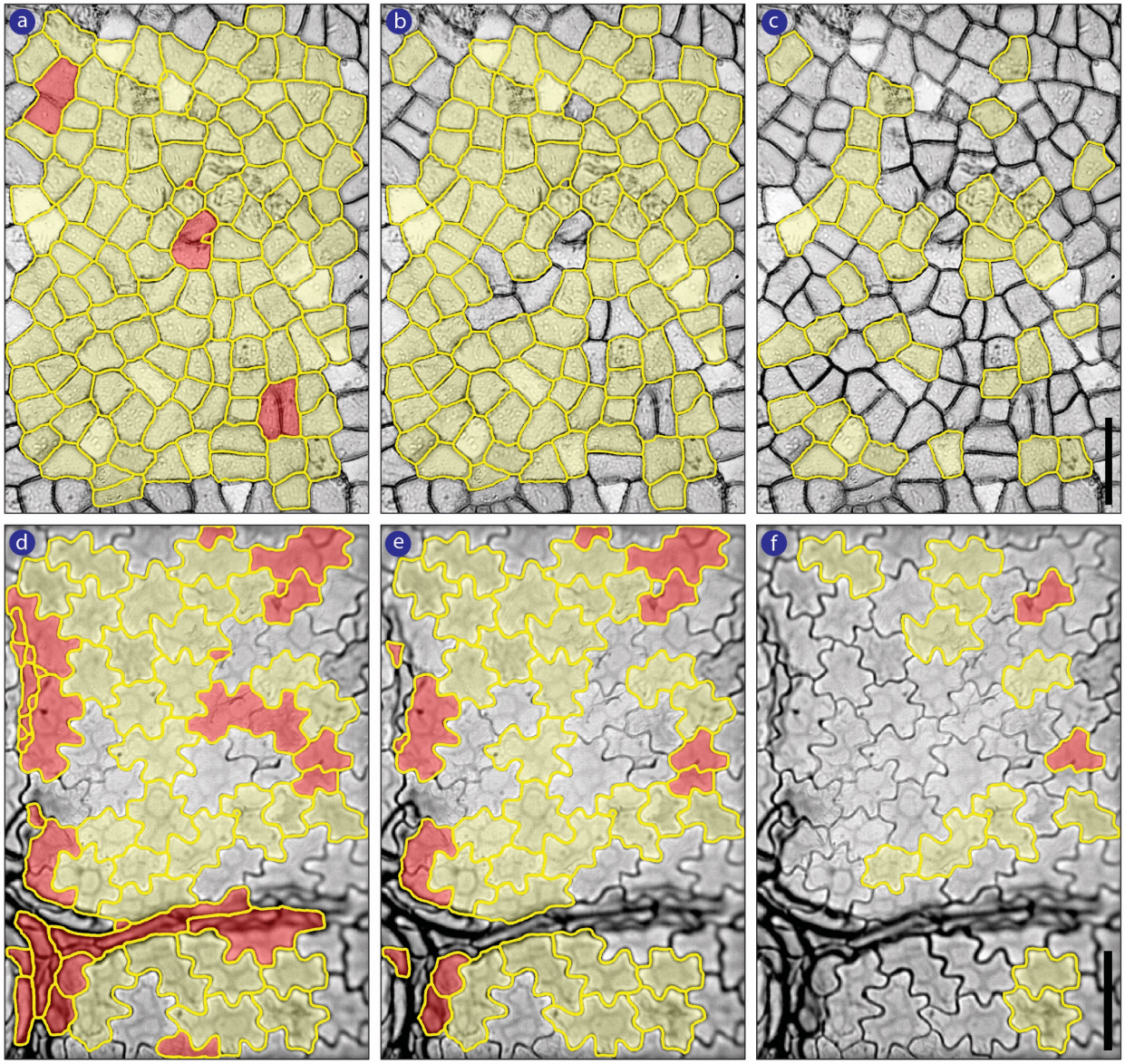

Fig. 3 Removal of unwanted ROIs by filtering with median statistics. **(a-c)** *Ocotea tarapotana* - Lauraceae, FLMNH00185; **(d-f)** *Acer skutchii* - Aceraceae, FLMNH00714. ROI sets that are **(a, d)** unfiltered, **(b, e)** ±2MAD-filtered, and **(c, f)** ±1MAD-filtered. Yellow outlines represent ROIs retained at each filtering level. Yellow-shaded ROIs accurately characterize epidermal pavement cells. Red-shaded ROIs do not accurately characterize pavement cells and are thus not wanted in the final dataset. Scale bars are 50 µm.

2.4 | Data Visualization

The "Batch Overlay" FIJI macro allows users to visualize CuticleTrace outputs by creating images overlain with outlines of each ROI in an ROI set, formatted to the user's preference. "Batch Overlay" may be used to overlay any batch of ROI sets on any batch of images. In our evaluation, we used "Batch Overlay" to visually check the accuracy of ROIs resulting from different input

parameters (Fig. 2) and to compare unfiltered ROI sets with the filtered versions from the "CuticleTrace Data Filtration" R Notebook (Fig. 3, 4).

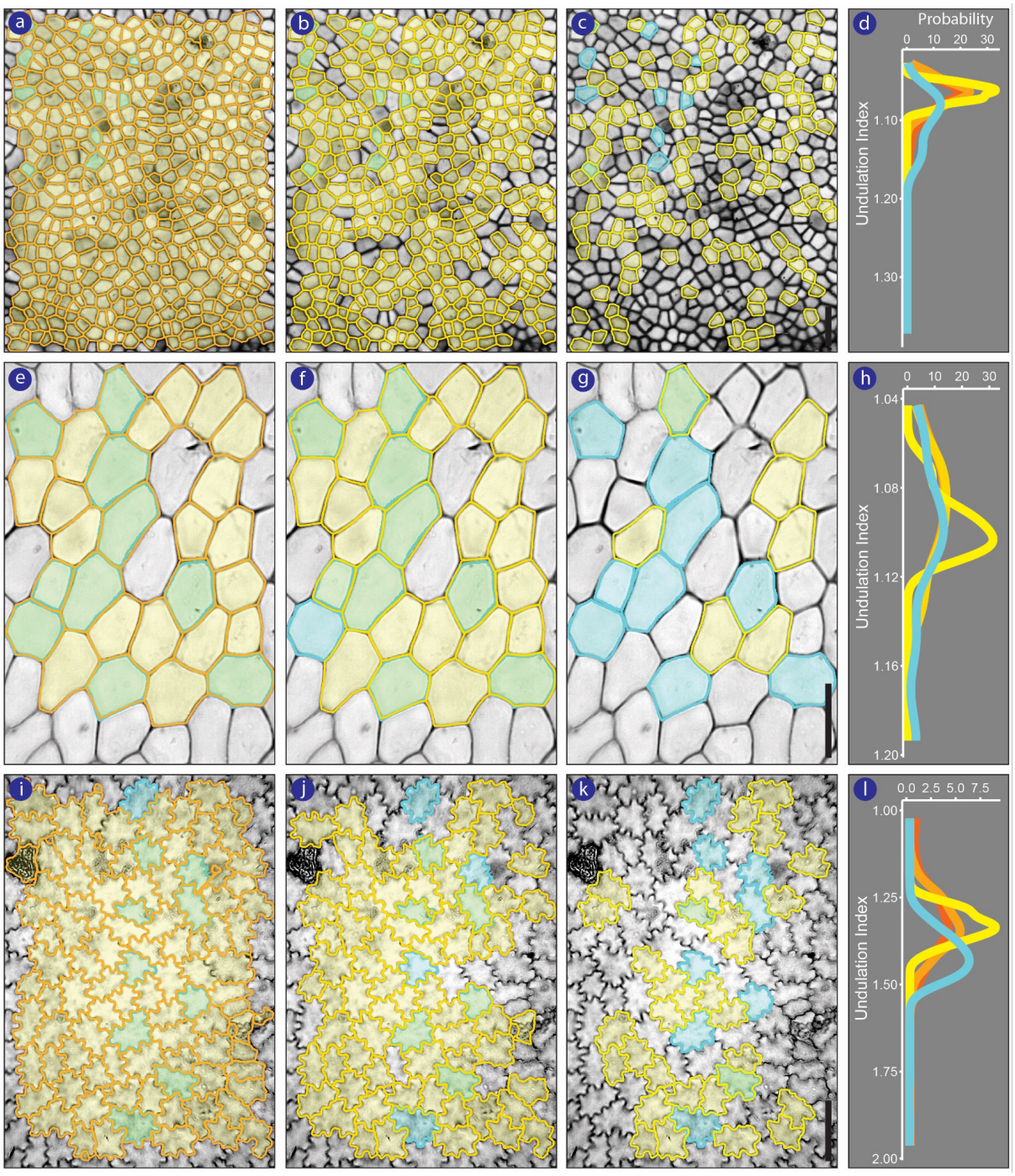

Fig. 4 CuticleTrace-generated ROI sets (yellow) compared to expert hand drawn ROI sets (cyan), with subsequent filtering using median statistics. Columns show ROI sets that are unfiltered **(a, e, i)**, ±2MAD **(b, f, j)**, and ±1MAD, overlain on the source images of **(a-c)** *Nectandra oppositifolia* - Lauraceae, FLMNH00260; **(e-g)** *Guarea bijuga* - Meliaceae, FLMNH00850, and **(i-l)** *Anaxagorea petiolata* - Annonaceae, FLMNH02589. **(d, h, l)** probability density plots showing distributions of Undulation Index values across all 4 datasets

for each image; hand-traced - cyan, unfiltered - dark orange, ±2MAD - light orange, ±1MAD - yellow. Scale bars are 50 µm.

3 | Evaluation and Results

3.1 | Dataset

We evaluated CuticleTrace across a range of image resolutions, magnifications, and qualities, using an image set of 50 vouchered herbarium specimens from the Cuticle Database (cuticledb.eesi.psu.edu, Barclay et al., (2007)). Images were chosen to maximize taxonomic breadth (48 species, 37 genera, 20 families) and span the range of cell shapes and sizes (Dataset S2).

We compared four sets of measurements for each image: CuticleTrace measurements following the protocol outlined in Methods S1, with user inputs specified in Table 2; hand-traced outlines of ten cells followed Dunn et al. (2015), traced by an expert (R.E.D) and University of Wyoming undergraduates (A.I.M, K.S.); and measurements generated by alternate automated methods (LeafNet (Li et al., 2022) and PaCeQuant (Möller et al., 2017)). PaCeQuant did not successfully segment our light-microscopy images (unsurprising, as it was developed for confocal microscopy images), and was excluded from statistical comparisons of segmentation methods.

Table 2. CuticleTrace batch-processing inputs for our 50-image test dataset.

Input Parameter	Value
Cell Walls on Background	Dark on Light
Gaussian Blur σ	2 pixels
Thresholding Algorithm	Sauvola (Sauvola & Pietikäinen, 2000)
Initial Thresholding Radius	50 pixels
ROI Size Filter	500-50,000 pixels^2
Smoothing Value	5% of Fourier descriptors

3.5 | Comparison of Methods

3.5.1 | Whole Image Comparison

The expert outlines served as our evaluation benchmark. We ran a one-way Analysis of Variance (ANOVA) with post-hoc nonparametric Games-Howell analysis for each shape parameter for each image. We selected the Games-Howell test due to differing sample sizes between the four sets of measurements. We used CuticleTrace's "Batch Overlay" macro to visually compare CuticleTrace and expert tracings (**Dataset S2**).

Our analyses showed 100% statistical agreement between CuticleTrace measurements (at both ±1MAD and ±2MAD filtering levels) and expert measurements of area, perimeter, Feret's diameter, aspect ratio, and roundness (Fig. 5). We observed some variability in circularity, solidity, and UI measurements, which was expected due to their sensitivity to small tracing differences. CuticleTrace measurements consistently aligned more closely with expert measurements than expert measurements did with student and LeafNet measurements (Table 3).

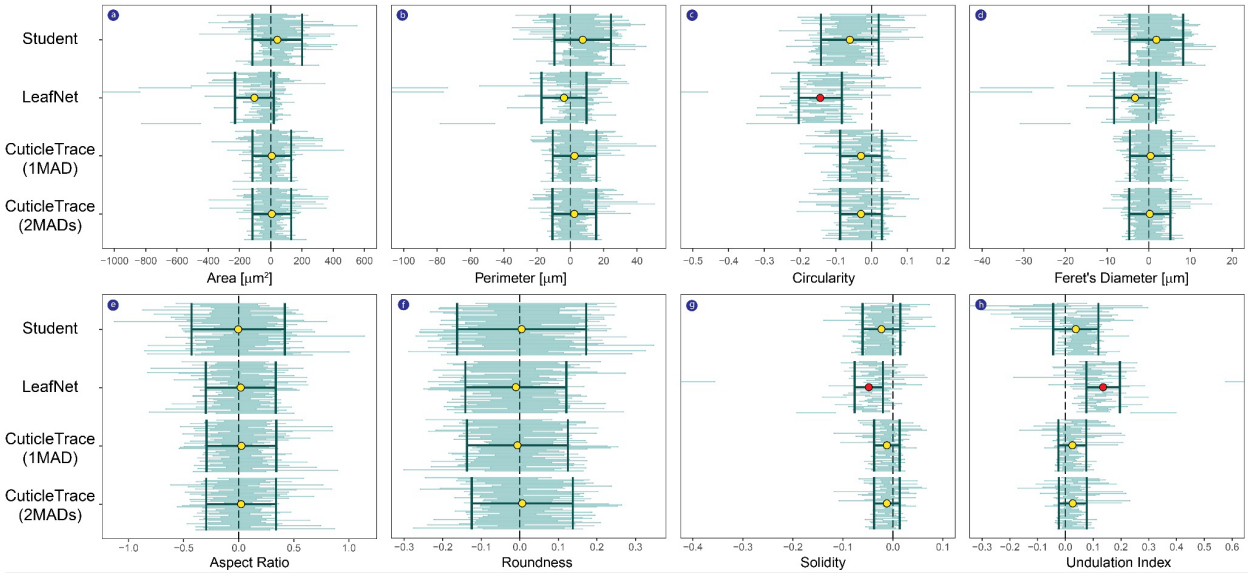

Fig. 5 Post-hoc Games-Howell results for all 50 images, separated by shape parameter. Comparisons are all relative to the hand-drawn expert results (zero). Student data was also hand-drawn; LeafNet and CuticleTrace are automated methods. Each small horizontal bar represents the 95% confidence interval of the Games-Howell mean difference estimate applied to a single image in the comparative dataset. The image position in the stack is maintained for each shape parameter. Darker bars with center circles are the mean ±2$\boldsymbol{\sigma}$ for each of the comparative stacks of Games-Howell results. Yellow center circles are non-significant; red center circles are significantly different from the expert.

Table 3. Statistical evaluation of ±1MAD and ±2MAD CuticleTrace measurements, student measurements, and LeafNet measurements, in comparison to expert measurements.

	Average Games-Howell p-value in comparison to Expert					% of measurements statistically identical to Expert (p-values >.05)				
	CuticleTrace					CuticleTrace				
Shape Parameter	±1MAD	±2MAD	Cell to Cell	Student	LeafNet	±1MAD	±2MAD	Cell to Cell	Student	LeafNet
Area	0.85	0.89	0.56	0.74	0.55	100	100	100	94	84
Perimeter	0.82	0.82	0.68	0.54	0.60	100	100	100	86	82
Feret's Diameter	0.85	0.88	0.64	0.66	0.72	100	100	100	94	88
Circularity	0.52	0.53	0.44	0.31	0.06	78	82	94	58	12
Aspect Ratio	0.79	0.82	0.88	0.75	0.81	100	100	100	100	100
Roundness	0.78	0.82	0.88	0.81	0.78	100	100	100	100	100
Solidity	0.44	0.47	0.42	0.34	0.18	76	78	90	72	30
Undulation Index	0.52	0.53	0.44	0.25	0.06	82	88	94	52	12
Mean	0.70	0.72	0.62	0.55	0.47	92.0	93.5	97.3	82.0	63.5

3.5.2 | Cell to Cell Comparison

We also completed a one-to-one comparison of CuticleTrace and expert measurements of individual cells (447 cells across all 50 images), which showed broad agreement across all shape

parameters (Fig. 6). In only 11 of 400 image measurements (50 images, eight shape parameters) were values significantly different at the 2-sigma level—a 2.75% error rate. Seven of the 11 significant differences are concentrated in three images—FLMNH00178 (*Damburneya salicifolia*), FLMNH00561 (*Gleditsia triacanthos*), and FLMNH05215 (*Pouteria durlandii*) (Fig. 6). However, overall, differences between expert and CuticleTrace tracings of the same cells were small, and CuticleTrace tracings were reasonable and consistent even when they differed from expert tracings.

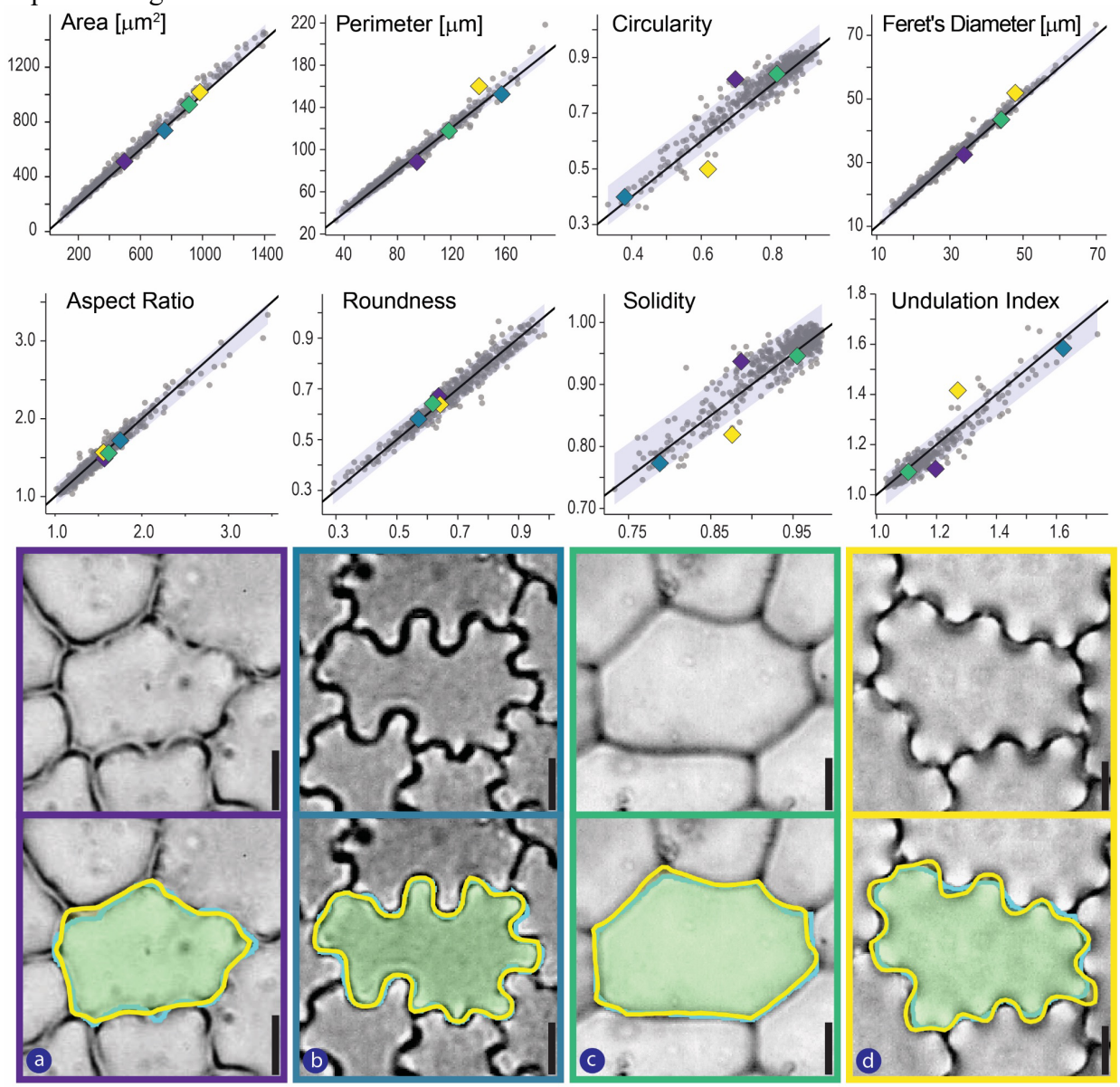

Fig. 6 Cell-to-cell comparison of Expert and CuticleTrace measurements. Upper panel: Correlation between Expert (x-axis) and CuticleTrace (y-axis) measurements across 447 cells and all relevant shape parameters, distributed between 50 images. Black lines have a slope of one, indicating 100% correlation. Shaded areas show 95% prediction intervals. Colored symbols correlate to the four images presented in the lower panel, which provides a visual comparison of the difference between cell outlines hand-drawn by an expert (cyan line) versus the CuticleTrace automated procedure (yellow line). Lower panel: (a) *Gleditsia triacanthos* - Fabaceae,

FLMNH00081; (b) *Toxicodendron striatum* - Anacardiaceae, FLMNH00510; (c) *Oreopanax capitatus* - Araliaceae, FLMNH00767; (d) *Pouteria durlandii* - Sapotaceae, FLMNH05215. Scale bars are 10 µm.

4 | Discussion

Consistent and accurate automated cell tracing is needed to enable high-throughput research that can disentangle the factors that influence epidermal morphology(Vőfély et al., 2019), and to apply known relationships between epidermal morphology and paleoenvironment (Dunn et al., 2015). The CuticleTrace toolkit streamlines and automates the segmentation and measurement of leaf epidermal pavement cells across a wide range of cell morphologies and image qualities.

4.1 | Accuracy of CuticleTrace Measurements

Across the wide range of cell shapes and image qualities encapsulated in our test dataset (**Dataset S2**), CuticleTrace produces cell shape measurements that are statistically identical to expert measurements across all shape parameters in most instances, at both the ±1MAD and ±2MAD filtering level. The limited, often non-significant, differences between expert and CuticleTrace measurements may be attributed to two sources of variation. First, the set of cells outlined by CuticleTrace may differ from those traced by an expert in the same image. However, *CuticleTrace* generates a much larger cell measurement dataset than is possible by hand. Therefore, provided the cells selected by CuticleTrace are representative of the whole image, the differences between the two methods were more likely a result of bias in the hand-drawn cells, as the grid-selection method of hand tracing results in smaller sample sizes and tends to favor larger cells.

Second, CuticleTrace may emphasize different aspects of cell morphology than an expert. Crenulated cells with obvious three-dimensional morphology showed the greatest number of disagreements (Fig. 6a, 6d). In these images, the expert chose to outline the cell wall at an alternate focal level from the CuticleTrace macros. The choice of focal level is somewhat subjective, however, and CuticleTrace's interpretation of the cell outline was largely reasonable and consistent. Our cell-to-cell comparison of 447 individual cells across 50 images showed that expert and CuticleTrace measurements are highly correlated (Fig. 6). For most images, CuticleTrace and expert measurements were effectively interchangeable.

The ease of data visualization built into CuticleTrace with the "Batch Overlay" and "Single Image Processor" macros is an important feature for ensuring accurate cell tracing and ROI filtering. Our design makes qualitative assessment of outputs easy, so that users can visually check all CuticleTrace outputs—thresholded images, skeletonized images, and filtered and unfiltered ROI sets—and modify input parameters as necessary. Additionally, CuticleTrace users may modify the "CuticleTrace Data Filtration" R notebook to suit their needs, and ROI sets may always be manually revised in FIJI.

Slide preparation, image quality, and CuticleTrace input parameters were the most important factors in ensuring accuracy in automated measurements. While we intentionally included a wide range of image qualities in our dataset (**Dataset S2**), we did not attempt to analyze Cuticle Database images that were of very poor quality. CuticleTrace's flexibility allows it to be fine-tuned for a wide variety of image preparations and resolutions, but that same flexibility may lead to ineffective or inaccurate image characterization if users neglect to carefully select input

parameters (Fig. 2). It is imperative that users closely follow instructions in the CuticleTrace User Manual (**Methods S1**).

5.2 | Comparison to Alternate Automated Methods

CuticleTrace is a unique addition to the suite of available methodologies for automatically segmenting and characterizing leaf epidermal morphology. Other approaches—PaCeQuant (Möller et al., 2017) and LeafNet (Li et al., 2022)—also automate epidermal pavement cell segmentation, with some limitations. Many other methods focus on stomata detection and characterization (e.g. Fetter et al., 2019; Li et al., 2022). Additional methods have been developed to trace cells in other plant tissues (Wolny et al., 2020) and more generally (Stringer et al., 2021).

Of these methods, CuticleTrace is the first to effectively trace and measure epidermal pavement cells across a wide variety of taxa, cell morphologies, and image qualities. The customizability of the "Batch Generate ROIs" and "Single Image Processor" FIJI macros allows users to tune CuticleTrace's settings to work well for their images. Unlike machine-learning approaches to cell segmentation, CuticleTrace does not require training images and can work with a broad range of morphologies with existing FIJI tools. It can therefore be more easily applied to studies involving diverse samples, detrital cuticle, or extinct taxa.

6 | Conclusions

The leaf epidermis contains a wealth of information about plants' evolutionary history and growth environments, and CuticleTrace makes that information significantly more accessible. In both living and fossil plants, epidermal pavement morphology can be utilized to gain insight into plant physiology, ecology, and evolution, and fossil evidence of epidermal cells are integral to some paleoenvironmental studies. The largest barrier to big-data approaches to these questions is the non-trivial task of accurately segmenting epidermal cell images. CuticleTrace represents a significant advance, greatly lowering the barrier to high-throughput studies of epidermal morphology by increasing the consistency of epidermal cell measurements and by vastly decreasing the labor investment required to generate cell shape datasets.

Acknowledgements

RSB acknowledges financial support from NSF grant EAR:1805228. SWP acknowledges support from a 2022 University of Illinois National Center for Supercomputing Applications (NCSA) Faculty Fellowship. EDC, RED, and AIM acknowledge support from NSF grant EAR:145031. BAL acknowledges financial support from Caroline Strömberg and thanks her, Alex Lowe, and Elena Stiles for constructive discussion.

Author contributions

BAL, RSB, RED and SWP conceived the study. BAL conducted the data analysis and created the FIJI image processing macros and 'R' filtering code. RED and AIM provided manual cell outlines. RED and EDC recruited and supervised the University of Wyoming students. BAL and SWP wrote the manuscript with help from RSB and RED. RSB and SWP supervised and directed the research.

Data availability

All generated and analyzed data from this study are included in the published article and its Supporting Information (**Dataset S2**). The code for the FIJI macros as well as the R notebook for filtering cells is available in the GitHub repository: (https://github.com/benjlloyd/CuticleTrace).

Supporting Information

Methods S1 – A detailed illustrated user manual for the CuticleTrace toolkit.
Dataset S2 – Images of ROI outputs from CuticleTrace (Unfiltered, ±1MAD, ±2MAD) and expert hand-tracing on all 50 images in our test dataset.

ORCID

Richard S. Barclay: https://orcid.org/0000-0003-4979-6970
Ellen D. Currano: https://orcid.org/0000-0002-5242-8573
Regan E. Dunn: https://orcid.org/0000-0002-6042-0619
Benjamin A. Lloyd: https://orcid.org/0000-0001-6749-2386
Surangi W. Punyasena: https://orcid.org/0000-0003-2110-5840

References

Barclay, R., Mcelwain, J., Dilcher, D., & Sageman, B. (2007). The Cuticle Database: Developing an interactive tool for taxonomic and paleoenvironmental study of the fossil cuticle record W. *CFS Courier Forschungsinstitut Senckenberg*, *258*, 39–55.

Brown, M. J. M., & Jordan, G. J. (2023). No cell is an island: Characterising the leaf epidermis using epidermalmorph, a new R package. *New Phytologist*, *237*(1), 354–366. https://doi.org/10.1111/nph.18519

Bush, R. T., Wallace, J., Currano, E. D., Jacobs, B. F., McInerney, F. A., Dunn, R. E., & Tabor, N. J. (2017). Cell anatomy and leaf δ13C as proxies for shading and canopy structure in a Miocene forest from Ethiopia. *Palaeogeography, Palaeoclimatology, Palaeoecology*, *485*, 593–604. https://doi.org/10.1016/j.palaeo.2017.07.015

Dunn, R. E., Strömberg, C. A. E., Madden, R. H., Kohn, M. J., & Carlini, A. A. (2015). Linked canopy, climate, and faunal change in the Cenozoic of Patagonia. *Science*, *347*(6219), 258–261. https://doi.org/10.1126/science.1260947

Fetter, K. C., Eberhardt, S., Barclay, R. S., Wing, S., & Keller, S. R. (2019). StomataCounter: A neural network for automatic stomata identification and counting. *New Phytologist*, *223*(3), 1671–1681. https://doi.org/10.1111/nph.15892

Kürschner, W. M. (1997). The anatomical diversity of recent and fossil leaves of the durmast oak (Quercus petraea Lieblein/Q. pseudocastanea Goeppert)—Implications for their use as biosensors of palaeoatmospheric CO2 levels. *Review of Palaeobotany and Palynology*, *96*(1), 1–30. https://doi.org/10.1016/S0034-6667(96)00051-6

Li, S., Li, L., Fan, W., Ma, S., Zhang, C., Kim, J. C., Wang, K., Russinova, E., Zhu, Y., & Zhou, Y. (2022). LeafNet: A tool for segmenting and quantifying stomata and pavement cells. *The Plant Cell*, *34*(4), 1171–1188. https://doi.org/10.1093/plcell/koac021

McElwain, J. C., & Chaloner, W. G. (1996). The Fossil Cuticle as a Skeletal Record of Environmental Change. *PALAIOS*, *11*(4), 376–388. https://doi.org/10.2307/3515247

Milligan, J. N., Flynn, A. G., Wagner, J. D., Kouwenberg, L. L. R., Barclay, R. S., Byars, B. W., Dunn, R. E., White, J. D., Zechmann, B., & Peppe, D. J. (2021). Quantifying the effect

of shade on cuticle morphology and carbon isotopes of sycamores: Present and past. *American Journal of Botany*, *108*(12), 2435–2451. https://doi.org/10.1002/ajb2.1772

Möller, B., Poeschl, Y., Plötner, R., & Bürstenbinder, K. (2017). PaCeQuant: A Tool for High-Throughput Quantification of Pavement Cell Shape Characteristics. *Plant Physiology*, *175*(3), 998–1017. https://doi.org/10.1104/pp.17.00961

R Core Team. (2022). *R: A Language and Environment for Statistical Computing*. R Foundation for Statistical Computing. https://www.R-project.org/

Royer, D. L. (2001). Stomatal density and stomatal index as indicators of paleoatmospheric CO2 concentration. *Review of Palaeobotany and Palynology*, *114*(1), 1–28. https://doi.org/10.1016/S0034-6667(00)00074-9

Schindelin, J., Arganda-Carreras, I., Frise, E., Kaynig, V., Longair, M., Pietzsch, T., Preibisch, S., Rueden, C., Saalfeld, S., Schmid, B., Tinevez, J.-Y., White, D. J., Hartenstein, V., Eliceiri, K., Tomancak, P., & Cardona, A. (2012). Fiji: An open-source platform for biological-image analysis. *Nature Methods*, *9*(7), Article 7. https://doi.org/10.1038/nmeth.2019

Stringer, C., Wang, T., Michaelos, M., & Pachitariu, M. (2021). Cellpose: A generalist algorithm for cellular segmentation. *Nature Methods*, *18*(1), Article 1. https://doi.org/10.1038/s41592-020-01018-x

Strömberg, C. A. E. (2011). Evolution of Grasses and Grassland Ecosystems. *Annual Review of Earth and Planetary Sciences*, *39*(1), 517–544. https://doi.org/10.1146/annurev-earth-040809-152402

Vőfély, R. V., Gallagher, J., Pisano, G. D., Bartlett, M., & Braybrook, S. A. (2019). Of puzzles and pavements: A quantitative exploration of leaf epidermal cell shape. *New Phytologist*, *221*(1), 540–552. https://doi.org/10.1111/nph.15461

Wolny, A., Cerrone, L., Vijayan, A., Tofanelli, R., Barro, A. V., Louveaux, M., Wenzl, C., Strauss, S., Wilson-Sánchez, D., Lymbouridou, R., Steigleder, S. S., Pape, C., Bailoni, A., Duran-Nebreda, S., Bassel, G. W., Lohmann, J. U., Tsiantis, M., Hamprecht, F. A., Schneitz, K., … Kreshuk, A. (2020). Accurate and versatile 3D segmentation of plant tissues at cellular resolution. *ELife*, *9*, e57613. https://doi.org/10.7554/eLife.57613

Zhao, C., Zhang, Y., Du, J., Guo, X., Wen, W., Gu, S., Wang, J., & Fan, J. (2019). Crop Phenomics: Current Status and Perspectives. *Frontiers in Plant Science*, *10*. https://www.frontiersin.org/articles/10.3389/fpls.2019.00714